Paper No.
05295

CORROSION2005

IRON CARBONATE SCALE FORMATION AND CO_2 CORROSION IN THE PRESENCE OF ACETIC ACID

Omkar A. Nafday and Srdjan Nesic

Institute for Corrosion and Multiphase Technology, Ohio University
342 West State Street
Athens, OH 45701

ABSTRACT

The role of acetic acid (HAc) on X-65 mild steel carbon dioxide (CO_2) corrosion has been investigated in the presence of iron carbonate scale ($FeCO_3$). Free HAc is known to be a source of hydrogen ions and to lead to an increase in mild steel corrosion rates, especially at low pH values. Protective iron carbonate scales form at high temperatures (>60°C) and high values of pH. An interesting situation occurs when free HAc and protective $FeCO_3$ scale co-exist. Numerous studies have looked at HAc and $FeCO_3$ scale effects separately, but there is little knowledge of how the protectiveness of $FeCO_3$ scale will be affected, in the presence of acetic acid. Some reports suggested $FeCO_3$ scale thinning and loss of protection in the presence of HAc Thus in order to clarify this aspect of CO_2 corrosion, the effect of HAc on $FeCO_3$ scale protectiveness using 3 wt % NaCl salt solution at T = 80°C has been studied under stagnant conditions. No effect of HAc on $FeCO_3$ scale protectiveness was found over a range of pH and HAc concentrations.

Keywords: Acetic acid, iron carbonate scale, X-65 mild steel, carbon dioxide, rotating cylinder electrode (RCE), super saturation, linear polarization method (LPR), scanning electron microscopy (SEM), x-ray diffraction (XRD)

INTRODUCTION

CO_2 is present in water as a dissolved gas under the high pressures common in underground oil and gas reservoirs. In the dissolved state it forms carbonic acid. The primary material of construction for pipelines in the oil and gas industry is mild steel, because of its price, strength and availability. However carbon steel corrodes in the presence of carbonic and organic acids such as acetic acid. It is therefore important to investigate the conditions in which HAc

causes corrosion damage to mild steel. The extent of HAc/CO_2 corrosion depends on many other variables such as: temperature, CO_2 partial pressure, pH, flow regime, etc.

Acetic acid corrosion: Carbon dioxide (CO_2) corrosion in the presence of acetic acid (HAc) has been the subject of numerous studies recently. These include laboratory work using cyclic voltametry[1,2], potentiodynamic sweeps[3,4] electrochemical impedance spectroscopy[5,6,7] in model systems and corrosion experiments using field brines[8,9,10]. As early as 1983, Crolet and Bonis[11] reported that the presence of acetic acid in the brine could increase the corrosion rate of carbon steel significantly. In the laboratory, HAc was found to greatly increase mild steel CO_2 corrosion rates at pH 4 (particularly at higher temperature) while the effect all but vanished at pH6 and higher. This can easily be explained by looking at the dissociation of HAc (which is a weak acid).

$$HAc \Leftrightarrow H^+ + Ac^- \tag{1}$$

The equilibrium constant for HAc dissociation, K_{HAc} is:

$$K_{HAc} = \frac{[H^+][Ac^-]}{[HAc]} \tag{2}$$

and depends on temperature as expressed by Kharaka[12]:

$$K_{HAc} = 10^{-(6.66104 - 0.0134916*T_k + 2.37856*10^{-5}*T_k^{\,2})} \tag{3}$$

The concentration of hydrogen ions, $[H^+]$ i.e. the pH determines the distribution of the acetic species in the solution i.e. how much is present in undissociated form and how much exists as acetate ion Ac^-. Thus, at different pH values, different amounts of undissociated (free) HAc can be found in the solution as shown in Table 1.

TABLE 1: ACETIC ACID SPECIES DISTRIBUTION AT VARIOUS pH VALUES, 80°C.

Total HAc added/ (ppm)	pH	Free [HAc] / (%)	[Ac^-] / (%)
1000	4	88	12
1000	5	58	42
1000	6	6.8	93.2
1000	6.6	1.8	98.2

As it was clearly established in the past[5,6,7] that the main cause of mild steel corrosion is the undisocciated (free) HAc and not the acetate ion (Ac^-), it is clear that the presence of organic acids is a major corrosion concern at lower pH. The distribution of acetic species with pH shown in Table 1 also explains while in some previous studies the CO_2 corrosion rate increased when acetic species were added as acetic acid (this reduced the pH) and why the CO_2 corrosion rate decreased when they were added as sodium acetate (this increased the pH). Therefore one is tempted to conclude that at a high pH, such as pH 6.6, there should be no effect on CO_2 corrosion since almost 98% of the acetic species is present as acetate ion (Ac^-). While this is generally true, there is a concern that the presence of organic acids somehow impairs the formation and protectiveness of iron carbonate ($FeCO_3$) scales.

Iron carbonate scale formation: Iron carbonate ($FeCO_3$) is one of the main corrosion products in the CO_2 corrosion process. Solid $FeCO_3$ forms on the steel surface if the product of ferrous ion concentration (Fe^{2+}) and carbonate ion concentration (CO_3^{2-}) exceeds the solubility product limit according to the reaction:

$$Fe^{2+} + CO_3^{2-} \Leftrightarrow FeCO_3(s) \tag{4}$$

The solubility product limit (Ksp_{FeCO3}) and supersaturation (SS) are related via:

$$SS = \frac{[Fe^{2+}][CO_3^{2-}]}{[Ksp_{FeCO_3}]} \tag{5}$$

The scale will precipitate when the SS value exceeds unity i.e. when the solution is supersaturated. The scale can be protective leading to the corrosion rate decrease. However, the rate of precipitation of iron carbonate can be so slow that the precipitation kinetics is more important in determining the protectiveness of the scale rather than the thermodynamics of the process. Johnson and Tomson[13] found that the most important factors which affect the precipitation of iron carbonate scale are supersaturation (SS) and temperature what lead them to propose a rate equation. A similar more frequently used expression for the rate of precipitation of the iron carbonate ($R_{FeCO_{3(s)}}$) is given by Van Hunnik et al.[14]

$$R_{FeCO_{3(s)}} = \frac{A}{V} \cdot f(T).K_{sp} \cdot f(SS) \tag{6}$$

where A is the surface area of the electrode and V the solution volume.

When iron carbonate precipitates at the steel surface, it decreases the corrosion rate by

- presenting a diffusion barrier for the species involved in the corrosion process;
- blocking a portion of the steel and preventing electrochemical reactions from occurring underneath it.

Although iron carbonate scale formation mechanisms and kinetics have been extensively studied[13-17] (thickness, morphology, porosity, etc.) its protectiveness in the presence of HAc is not known.

EXPERIMENTAL PROCEDURE

The experiments were performed in a two-liter glass cell. A schematic representation of the experimental setup is shown in Figure 1. All experiments were conducted at a given pH, and a fixed temperature, 80°C. In order to establish baseline results, experiments were started without HAc at pH 6.6, supersaturation values of SS=162 and SS=32 where iron carbonate scale formation is known to occur. These SS values were obtained by adding 50 and 10 ppm of Fe^{2+} respectively to the experiments in the form of ferrous chloride. These baseline results then served as a means of comparison with experiments in the presence of HAc. Typical experiments were conducted over a period of three days in order to see the stabilized corrosion rate. Table 2 outlines the experimental test matrix.

TABLE 2: TEST MATRIX

Parameter	*Value*
Steel type	X-65
Solution	3% NaCl
Gas	CO_2
pH	6.6
Free HAc (ppm)	0, 18, 72, 180
Temperature (°C)	80
Fe^{2+} (ppm)	10, 50
Rotational velocity (rpm)	0
Sand paper grit used	220, 400, 600
Measurement techniques	LPR, SEM, WL, XRD

Experimental procedure

The glass cell was filled with two liters of deionised (DI) water to which 3% by weight of NaCl salt was added. A 1 M KCl solution was used in a salt bridge connecting the reference electrode with the cell. The counter electrode (CE) used was a platinum ring concentric with the working electrode. CO_2 gas was used to deoxygenate the solution for at least an hour. Once deoxygenation has been achieved, HAc was added at the start of every experiment conducted in the presence of HAc. The pH of the solution was then adjusted to the desired value by adding sodium bicarbonate ($NaHCO_3$). It should be pointed out that the pH was maintained at the desired value throughout the experiment by minute addition of hydrochloric acid (HCl) or $NaHCO_3$ as needed. The desired concentration of Fe^{2+} was then added to the cell in the form of ferrous chloride $FeCl_2.4H_2O$ crystals pre-dissolved in deoxygenated DI water. Before introduction, the specimen was polished successively using 220, 400 and 600 grit sand paper. Since $FeCO_3$ scale precipitation is very surface sensitive, it was important to polish the metal coupon to a uniform finish in all the experiments in order to get reproducible results. A CO_2 gas preconditioning vessel and a condenser were used to minimize the loss of acetic acid from the test cell by evaporation. Regular monitoring of the Fe^{2+} concentration was done throughout the duration of the experiment. It must be stressed that the nominal Fe^{2+} concentration (50 or 10 ppm) and the corresponding supersaturation *SS* discussed in this paper represented only the initial value at the beginning of the experiment. As the experiment progressed, the Fe^{2+} concentration and *SS* decreased gradually due to iron carbonate precipitation. Fe^{2+} concentration less than 0.1 ppm was measured towards the end of the experiment and supersaturation tended toward unity. At the end of the test, the sample was removed from the cell and stored in a moisture free cabinet for SEM analysis of the scale and for visual inspection for any initiation of localized corrosion.

X-65 mild steel working electrode

The cylindrical working electrode was machined from the parent material and had a diameter of 0.012 m and an area of 5.4 cm^2. The composition of the X-65 specimen is as shown in Table 3.

TABLE 3: CHEMICAL COMPOSITION OF X-65 STEEL (wt %)

Al	As	B	C	Ca	Co	Cr	Cu	Mn	Mo	Nb	Ni	P	Pb	S
0.032	0.005	0.0003	0.05	0.004	0.006	0.042	0.019	1.32	0.031	0.046	0.039	0.013	0.02	0.002

Sb	Si	Sn	Ta	Ti	V	Zr	Fe
0.011	0.31	0.001	0.007	0.002	0.055	0.003	Balance

Experimental analysis

Linear polarization resistance (LPR) and weight loss (WL) were used to measure the corrosion rate. Scanning electron microscopy (SEM) and X-ray diffraction (XRD) were used to analyze the type and thickness of the scale formed. In order to test for localized corrosion and do SEM cross-section on the same sample, the scaled up sample was immersed only half-way in epoxy. The advantage of this method is that the metal surface could be examined for localized attack on one side (by removing the scale) and SEM analysis could be performed on the other side encased in epoxy without having to repeat experiments or have multiple samples for each of the two tasks. Figure 2 illustrates the metal sample encased halfway in epoxy and ready for cross-sectional analysis.

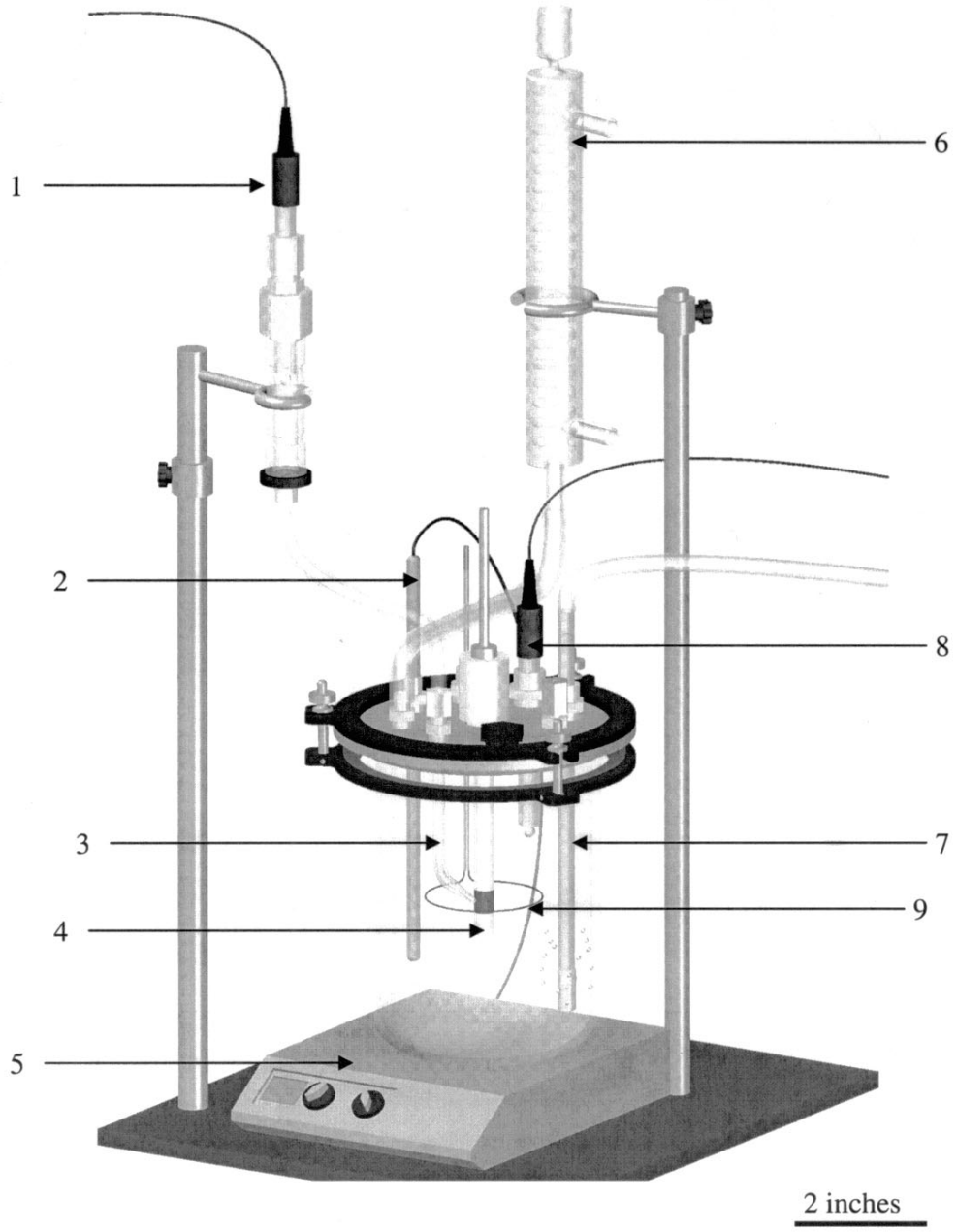

1. Reference electrode; 2. Temperature probe; 3. Luggin capillary; 4. Working electrode; 5. Hot plate; 6. Condenser; 7. Bubbler for gas; 8. pH electrode; 9. Counter electrode

FIGURE 1: Schematic of the glass cell setup.

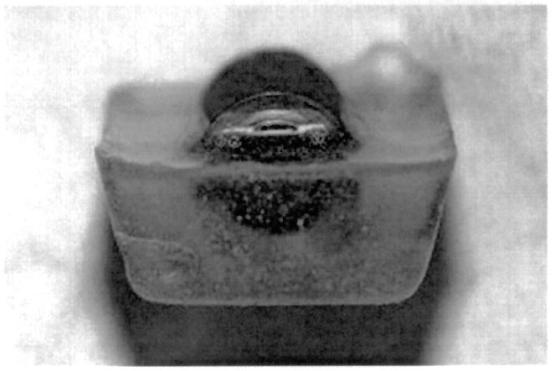

FIGURE 2: Sample encased halfway in epoxy

RESULTS

For clarity and better understanding of results, the presentation of the experimental results is arranged in the order of decreasing SS values. At each SS value, results at different free HAc concentrations are shown.

Baseline tests without HAc

Baseline experiments were conducted without HAc at 10 and 50 ppm Fe^{2+} at pH 6.6, to determine the corrosion rates and iron carbonate scale formation in the absence of HAc. Figure 3 shows the uniform corrosion rate curves for experiments without HAc at pH 6.6, 80°C, stagnant, with 50 and 10 ppm Fe^{2+}. As expected, it takes longer time for a protective scale to form at 10 ppm Fe^{2+} (SS = 32) than at 50 ppm Fe^{2+} (SS = 162). In both cases, a protective iron carbonate scale is formed and the corrosion rate drops rapidly from about 1.3 mm/yr to less than 0.1 mm/yr. This is also reflected in the iron (Fe^{2+}) counts taken towards the end of the experiment when they decreased to less than 0.1 ppm in both cases. Thus we see that in these two cases the change in the Fe^{2+} concentration (supersaturation) affects only the rate of scale formation, i.e. how fast a protective scale is formed but not its protectiveness.

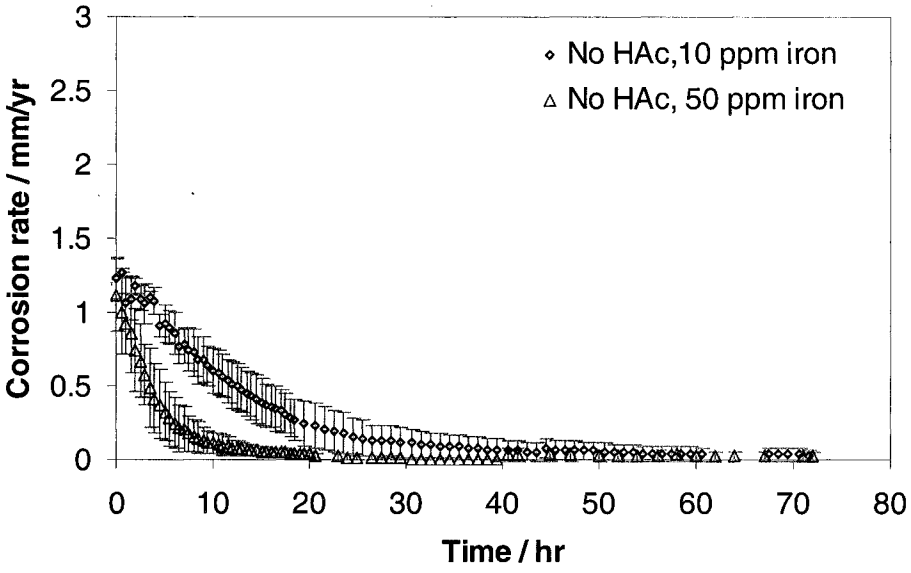

FIGURE 3: Uniform corrosion rate variation with time in experiments without HAc at pH 6.6, 80°C, 10 and 50 ppm Fe^{2+}, at stagnant conditions. Error bars represent the maximum and minimum values of corrosion rate observed in repeated experiments.

Supersaturation (SS) of 162

a) **<u>18 ppm free HAc</u>:**

Figure 4 shows the corrosion rate curves averaged over multiple experiments without and with 18 ppm free HAc (1000 ppm HAc total) at SS = 162, pH 6.6, 80°C, 50 ppm Fe^{2+}. Experiments were conducted without and with 18 ppm free HAc over 3 days until stable results were obtained. Results of three repeatable experiments without and with 18 ppm free HAc are shown. We see a higher starting corrosion rate in presence of HAc although HAc has no significant effect on the final corrosion rates. The corrosion rate curves of all experiments performed are shown in the logarithmic scale in Figure 5. We see a difference in the final corrosion rates of experiments although they do not have much significance as they are much less than 0.1 mm/yr. Figure 6a shows the front view pictures of the scale at 1500X magnification and also the optical microscope pictures at 600X with the scale removed to examine for localized attack. As seen from the optical microscope pictures in Figure 6b, there is uniform corrosion on the metal and no evidence of localized attack is observed. Figure 7 shows the SEM cross-section pictures at 500X. There is no differentiation possible between the thickness of scales formed without and with 18 ppm free HAc. The scales in both cases are 10-15 μm thick. The results show that presence of 18 ppm free HAc has no effect on scale thickness and protectiveness under these conditions.

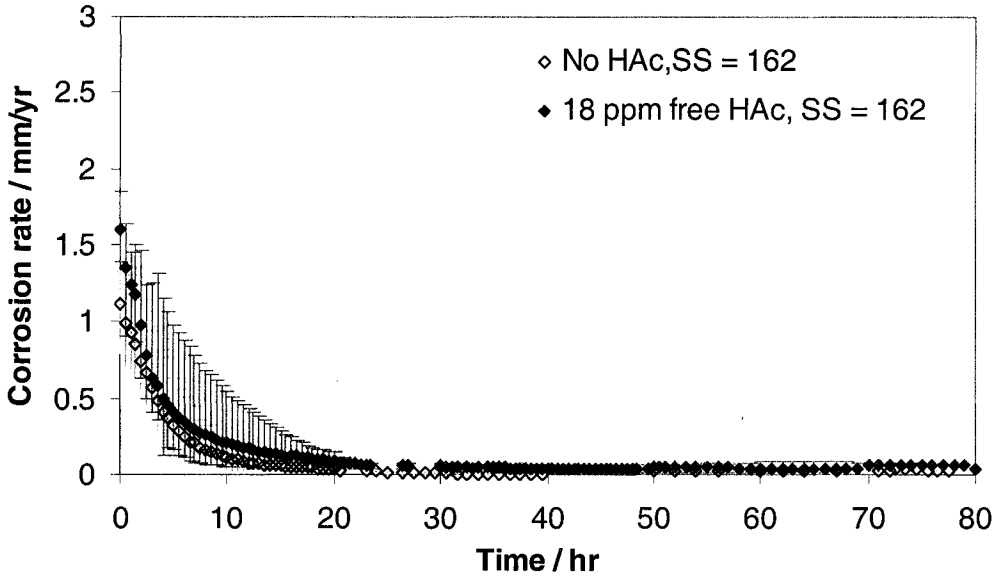

FIGURE 4: Uniform corrosion rate plot with time in experiments without and with 18 ppm free HAc (1000 ppm total) at SS = 162, pH 6.6, 80°C, 50 ppm Fe^{2+}. Error bars represent the maximum and minimum values of corrosion rate observed, refer to Figure 5 for the curves in the logarithmic scale, Figure 6 for SEM front view and Figure 7 for SEM cross-sectional view.)

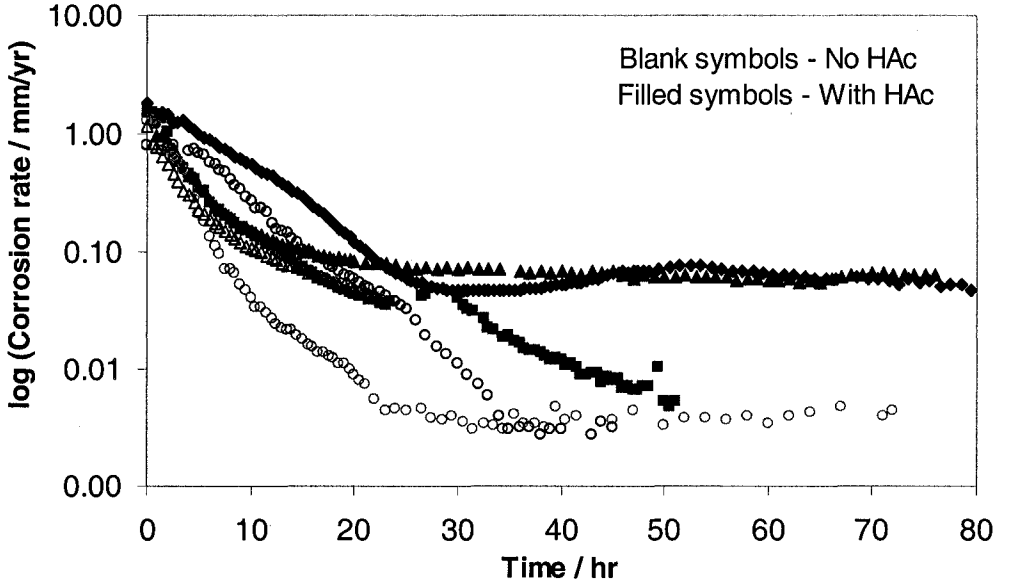

FIGURE 5: Uniform corrosion rate progression with time shown on a logarithmic scale at SS = 162, pH 6.6, T = 80°C, 50 ppm Fe^{2+}, without and with 18 ppm free HAc (1000 ppm total), stagnant conditions. (Refer to Figure 4 for the same curves shown on a linear scale, Figure 6 for SEM front view and Figure 7 for SEM cross-sectional view.)

a) SEM pictures (frontal view) at 1500 X

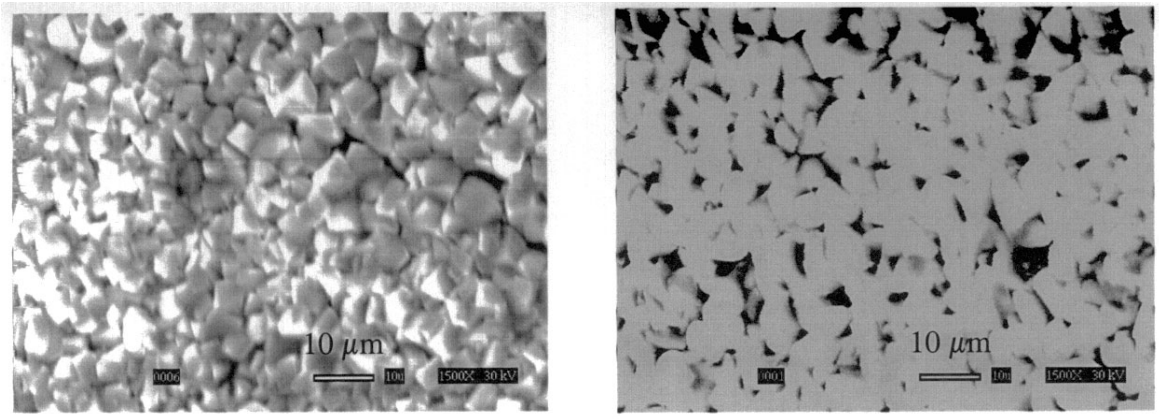

Without HAc

With 18 ppm free HAc

b) Optical microscope pictures at 600X

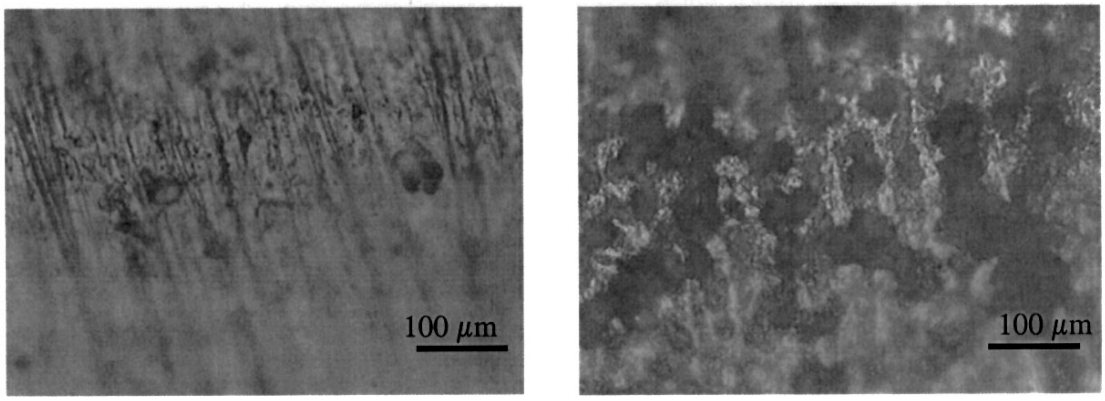

Scale removed (without HAc)

Scale removed (with 18 ppm free HAc)

FIGURE 6: Front view pictures of $FeCO_3$ film at SS = 162, pH 6.6, 80°C, 50 ppm Fe^{2+}, 18 ppm free HAc (1000 ppm total), stagnant condition. (Refer to Figure 4 for the average curves, Figure 5 for all curves in the logarithmic scale, Figure 7 for SEM cross-sectional view.)

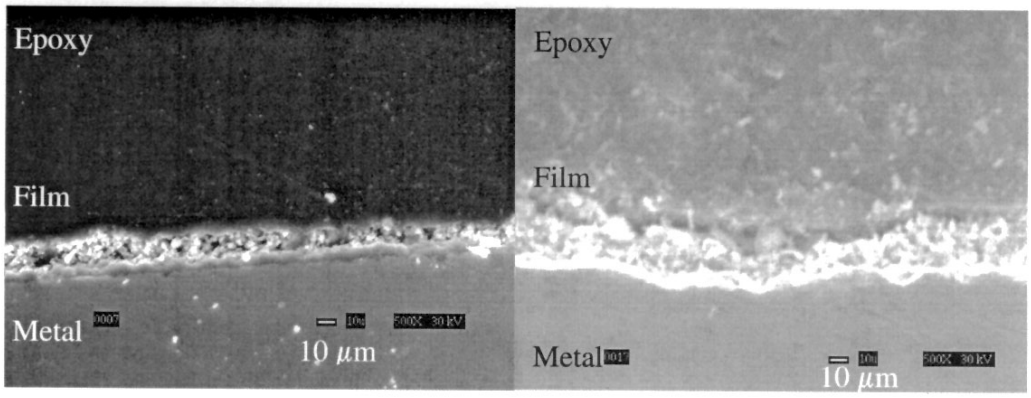

Without HAc With 18 ppm free HAc

FIGURE 7: SEM pictures (cross sectional view) of $FeCO_3$ scale at 500 X, SS = 162, pH 6.6, 80° C, 50 ppm Fe^{2+}, 18 ppm free HAc (1000 ppm total), stagnant condition. (Refer to Figure 4 for the uniform corrosion rate curves shown on a linear scale, Figure 5 for all curves in the logarithmic scale, Figure 6 for the front view.)

b) <u>72 ppm free HAc</u>:

Figure 8 shows the corrosion rate curves averaged over the multiple experiments without and with 72 ppm free HAc (4000 ppm HAc total) at SS = 162, pH 6.6, 80°C, 50 ppm Fe^{2+}. Experiments were conducted without and with 72 ppm free HAc over 3 days until stable results were obtained. We again see a higher starting corrosion rate in the presence of HAc although HAc has no significant effect on the final corrosion rates. The experimental curves of all experiments performed are shown on the logarithmic scale in Figure 9, which shows a slight difference in the corrosion rate progression. On examination of the front view pictures of the scale as shown in Figure 10a at 1500X we see that the size of the crystals with HAc is greater than those observed without HAc, although both offered the same protection. The optical microscope pictures with the scale removed as shown in Figure 10b show no evidence of localized attack. Figure 11 shows the SEM cross-section pictures at 500X. The scales in both cases are 15-25 μm thick. These results show that the presence of 72 ppm free HAc has no effect on scale thickness and protectiveness.

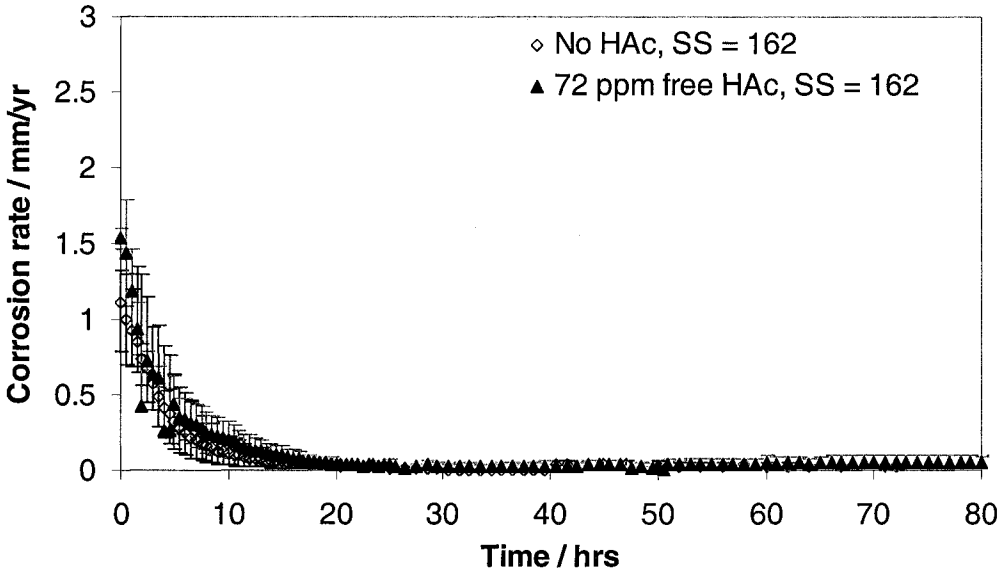

FIGURE 8: Uniform corrosion rate plot with time in experiments without and with 72 ppm free HAc (4000 ppm HAc total) at SS = 162, pH 6.6, 80° C, 50 ppm Fe^{2+}(Error bars represent the maximum and minimum values of corrosion rate observed, refer to Figure 9 for the curves in the logarithmic scale, Figure 10 for SEM front view and Figure 11 for SEM cross-sectional view.)

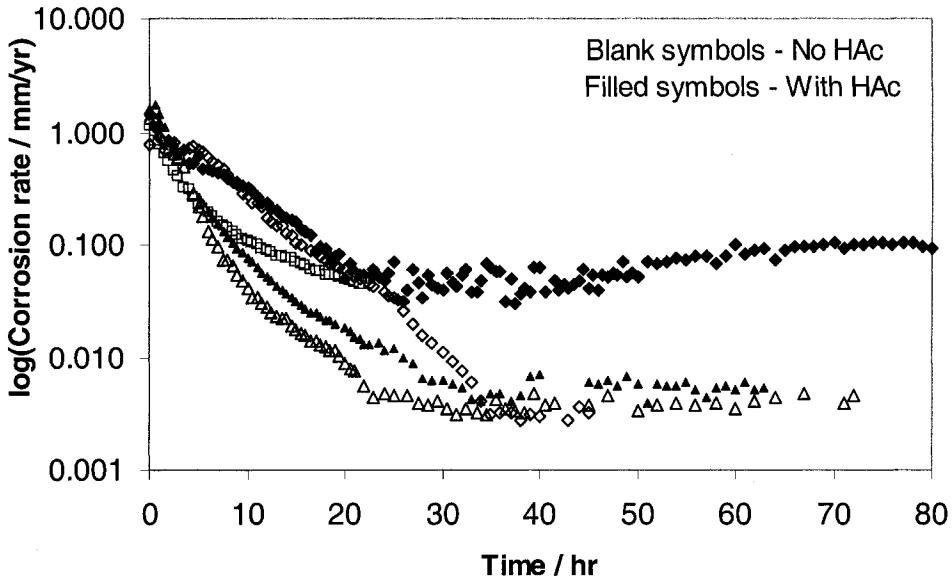

FIGURE 9: Uniform corrosion rate progression with time shown on a logarithmic scale at SS = 162, pH 6.6, T = 80°C, 50 ppm Fe^{2+}, without and with 72 ppm free HAc (4000 ppm HAc total), stagnant conditions. (Refer to Figure 8 for the same curves shown on a linear scale, Figure 10 for the front view and Figure 11 for SEM cross-sectional view)

a) SEM pictures (frontal view) at 1500 X

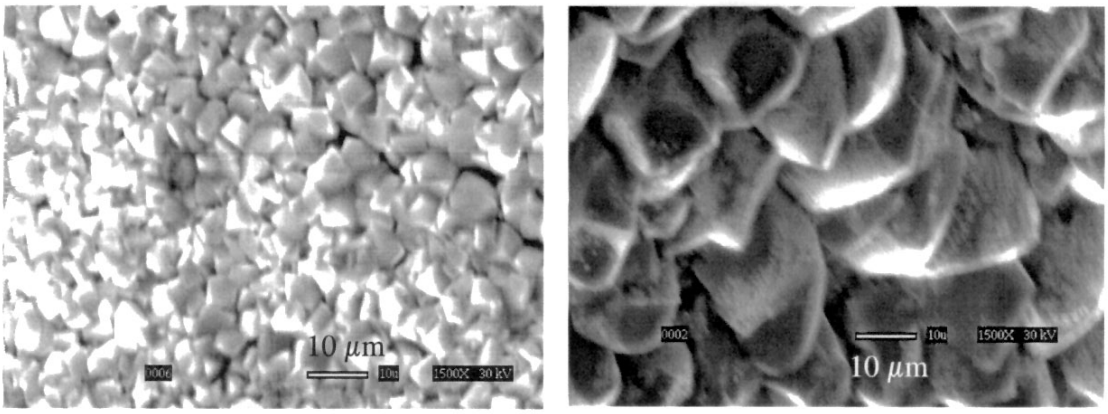

Without HAc

With 72 ppm free HAc

b) Optical microscope pictures at 600X

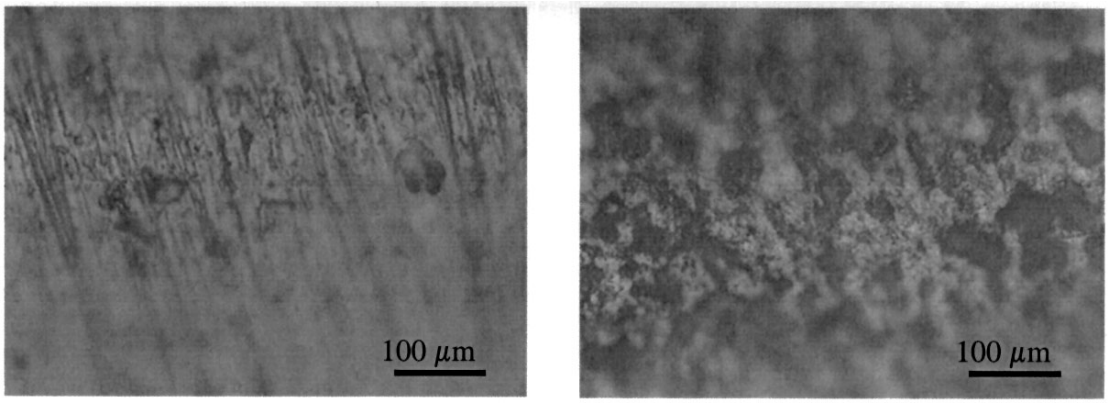

Scale removed (without HAc)

Scale removed (with 72 ppm free HAc)

FIGURE 10: Front view pictures of $FeCO_3$ film at SS = 162, pH 6.6, 80°C, 50 ppm Fe^{2+}, without and with 72 ppm free HAc (4000 ppm HAc total), stagnant condition. (Refer to Figure 8 for the average curves, Figure 9 for the curves in the logarithmic scale, Figure 11 for the cross-sectional view)

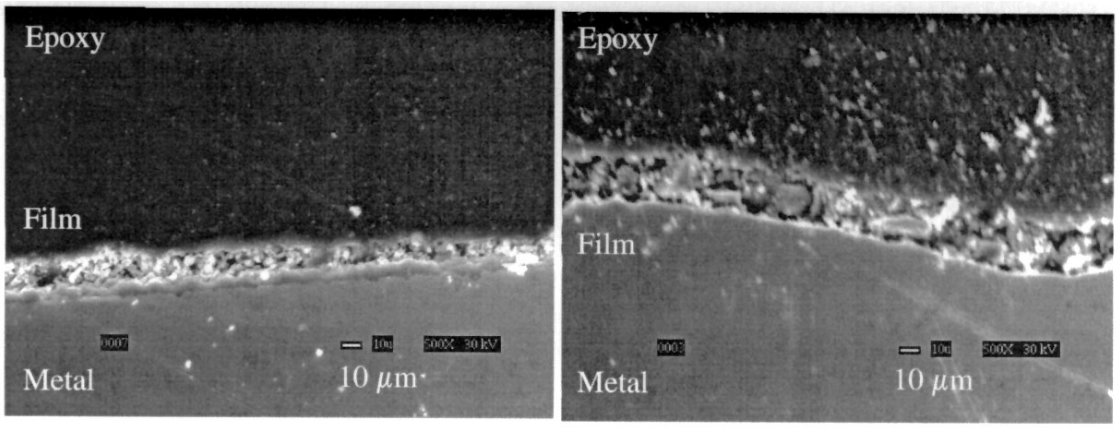

Without HAc With 72 ppm free HAc

FIGURE 11: SEM pictures (cross sectional view) of $FeCO_3$ scale at 500 X, SS = 162, pH 6.6, 80°C, 50 ppm Fe^{2+}, with 72 ppm free HAc (4000 ppm HAc total), stagnant condition. (Refer to Figure 8 for the uniform corrosion rate curves shown on a liner scale, Figure 9 for the curves on a logarithmic scale, Figure 10 for the front view.)

c) <u>180 ppm free HAc</u>:

Figure 12 shows uniform corrosion rate curves for experiments without and with 180 ppm free HAc (10,000 ppm HAc total) at pH 6.6, 80°C, 50 ppm Fe^{2+}. The starting corrosion rate with HAc is again higher than experiments without HAc although there is no effect on the final corrosion rates. The experimental curves of all experiments performed are shown on a logarithmic scale in Figure 13. There is again a slight variation in corrosion rates but it must be noted that these are insignificant as the small differences are exaggerated on the logarithmic scale and the final corrosion rate is the same. Figure 14a shows the front view pictures of the scale at 1500X and also with the scale removed at 600X to look for localized attack. The size of crystals with HAc is similar to those observed without HAc. We also see from the optical microscope pictures as in Figure 14b, there is no localized attack. Figure 15 shows the SEM cross-section pictures at 500X. Again the thicknesses of scales formed without and with HAc are identical. No effect of 180 ppm free HAc is seen on the structure or protectiveness of the iron carbonate scale.

Figure 16 shows the comparison of uniform corrosion rate change curves at SS = 162, without and with 18, 72 and 180 ppm free HAc over 3 days. We see a variation in the corrosion rates but there is no direct relation between HAc concentration and final corrosion rate, i.e in all cases the same protective iron carbonate film was observed irrespective of the free HAc concentration.

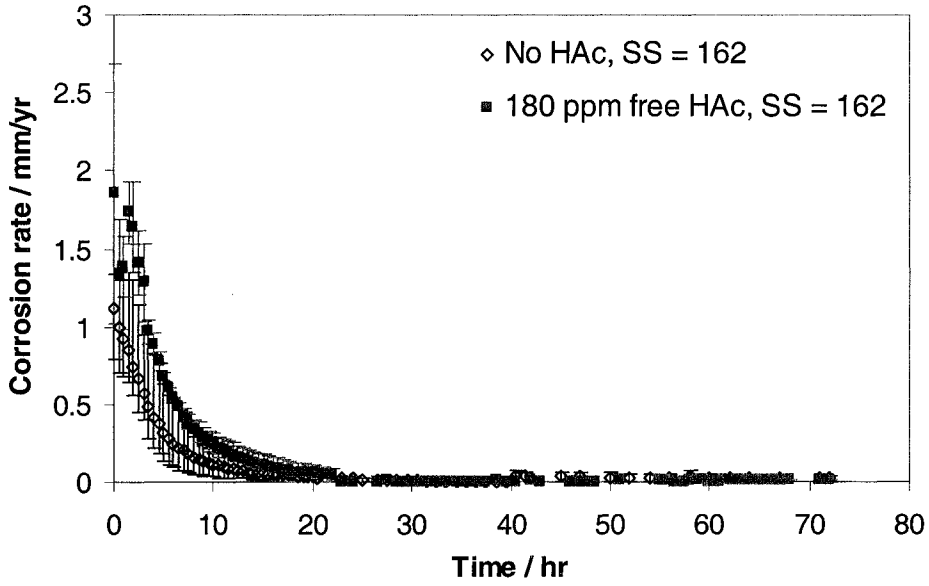

FIGURE 12: Uniform corrosion rate plot with time in experiments without and with 180 ppm free HAc (10,000 ppm HAc total) at SS = 162, pH 6.6, 80°C, 50 ppm Fe^{2+}(Error bars represent the maximum and minimum values of corrosion rate observed. Refer to Figure 13 for the curves in the logarithmic scale, Figure 14 for SEM front view and Figure 15 for SEM cross-sectional view.)

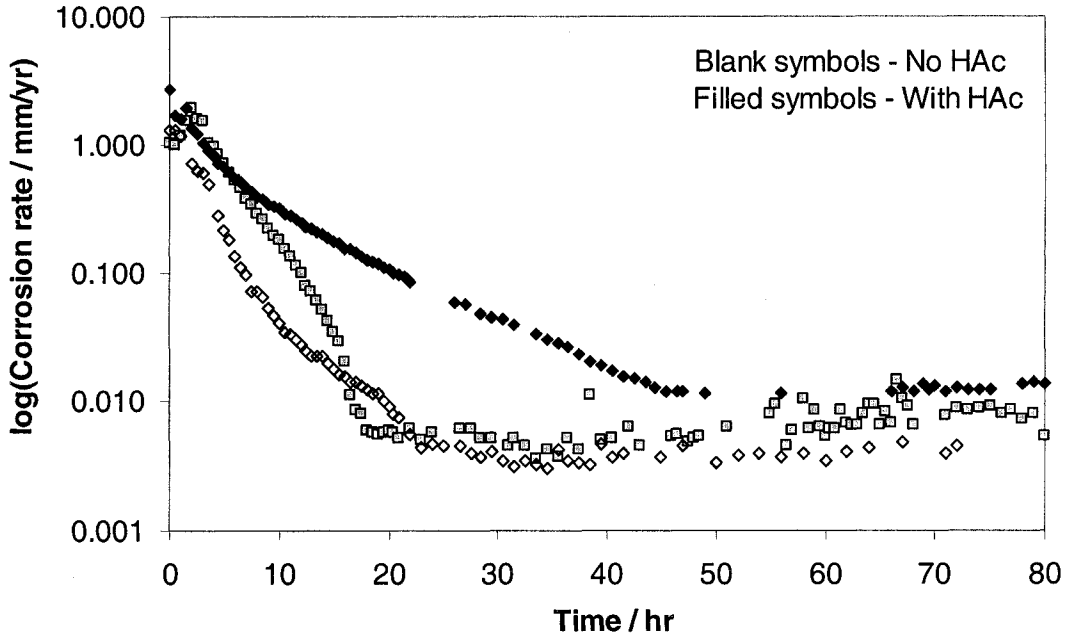

FIGURE 13: Uniform corrosion rate progression with time shown on a logarithmic scale at pH 6.6, T = 80°C, 50 ppm Fe^{2+}, without and with 180 ppm free HAc (10,000 ppm HAc total), stagnant conditions. (Refer to Figure 12 for the same curves shown on a linear scale, Figure 14 for SEM front view and Figure 15 for SEM cross-sectional view)

a) SEM pictures (frontal view) at 1500 X

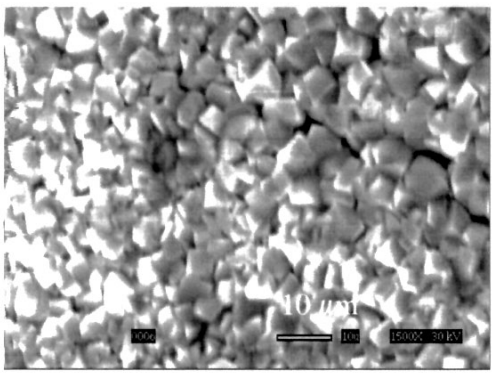

Without HAc

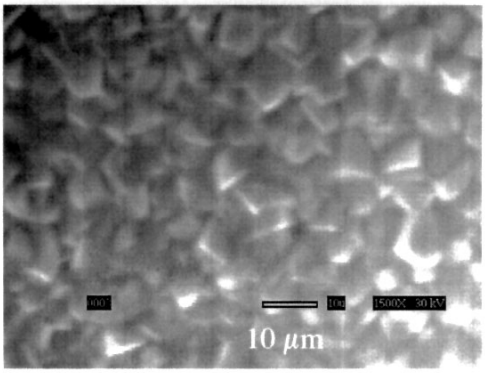

With 180 ppm free HAc

b) Optical microscope pictures at 600X

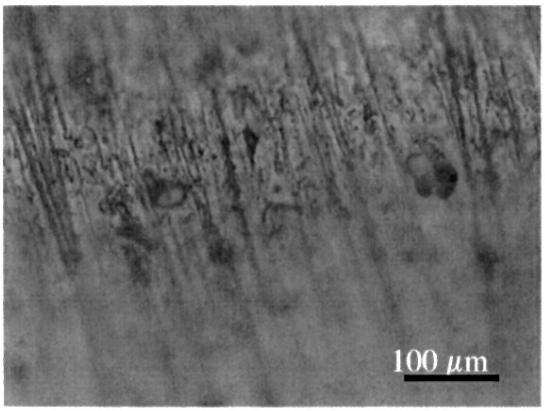

Scale removed (without HAc)

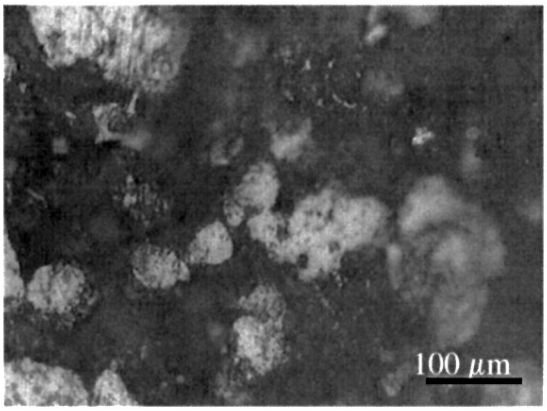

Scale removed (with 180 ppm free HAc)

FIGURE 14: Front view pictures of $FeCO_3$ film at SS = 162, pH 6.6, 80°C, 50 ppm Fe^{2+}, without and with 180 ppm free HAc (10,000 ppm HAc total), stagnant condition. (Refer to Figure 12 for the average curves, Figure 13 for the curves in the logarithmic scale, Figure 15 for SEM cross-sectional view)

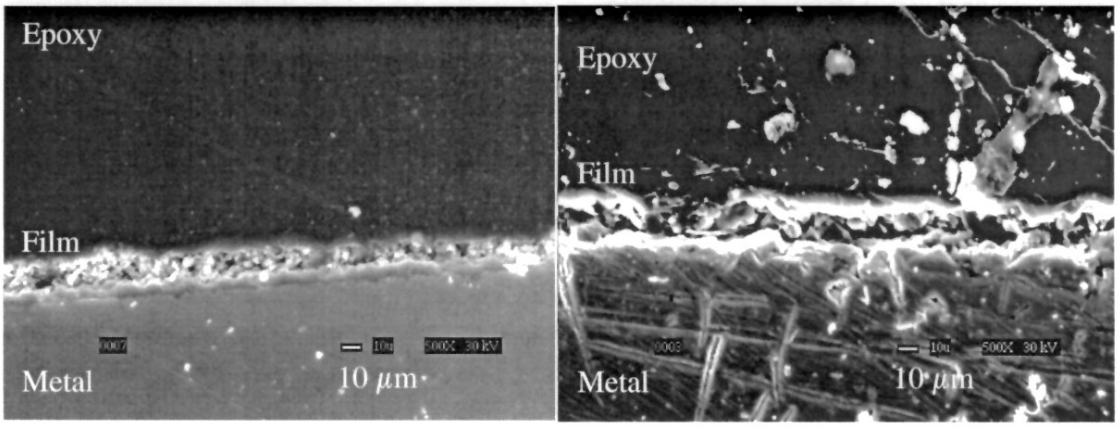

Without HAc With 180 ppm free HAc

FIGURE 15: SEM pictures (cross sectional view) of $FeCO_3$ scale at 500 X, SS = 162, pH 6.6, 80°C, 50 ppm Fe^{2+}, 180 ppm free HAc (10,000 ppm HAc total), stagnant condition. (Refer to Figure 12 for the uniform corrosion rate curves shown on a linear scale, Figure 13 for the curves on the logarithmic scale, Figure 14 for the front view at the same conditions)

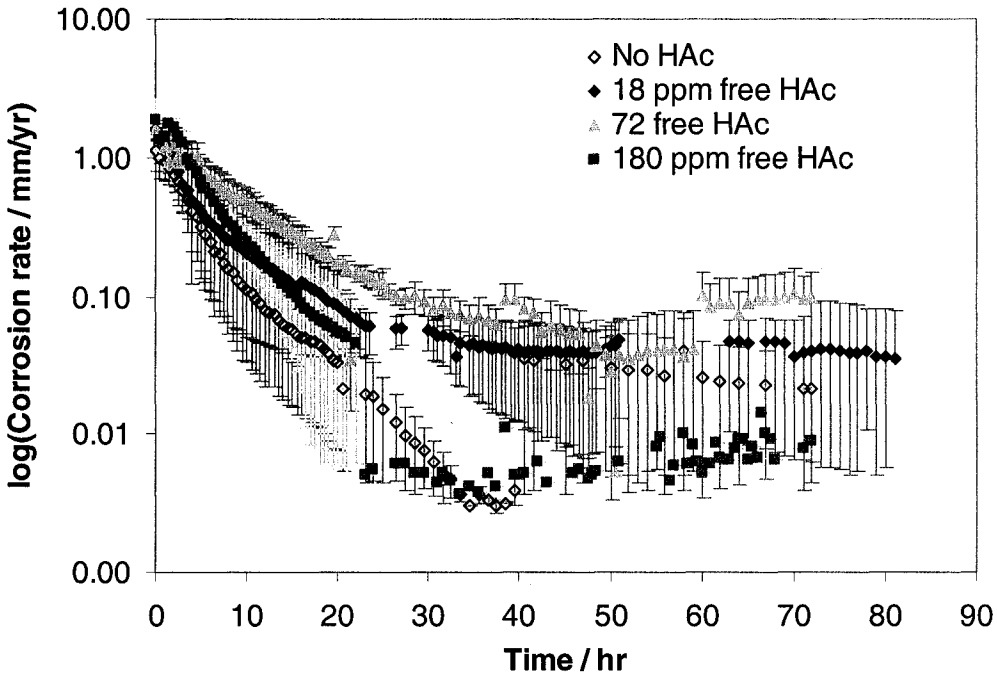

FIGURE 16: Comparison of the uniform corrosion rate curves at SS = 162, pH 6.6, 80°C, 50 ppm Fe^{2+}, with 18, 72 and 180 ppm free HAc, stagnant condition. (Error bars represent the maximum and minimum values of corrosion rates observed)

Supersaturation (SS) of 32

a) **<u>72 ppm free HAc</u>:**

Figure 17 shows uniform corrosion rate curves for experiments at SS = 32, pH 6.6, 10 ppm Fe^{2+}, stagnant condition without and with 72 ppm free HAc (4000 ppm HAc total), over 3 days. The protective scale took longer to form when compared to the previous series of experiments done at SS=162. From Figure 17 it is clear that there is no significant effect of HAc after 30 hours although the starting corrosion rates with HAc are higher. Refer to Figure 18 for the same data shown on a logarithmic scale. Figure 19a shows the front view pictures of the scale at 1500X and also with the scale removed at 600X to look for localized attack. The size of crystals is virtually the same when compared with and without HAc. There is no evidence of localized attack as seen from Figure 19b. Figure 20 shows the SEM cross-section pictures at 500X. Again the thicknesses of scales formed without and with HAc are similar. No effect of 72 ppm of free HAc on the free corrosion rate is observed under these conditions.

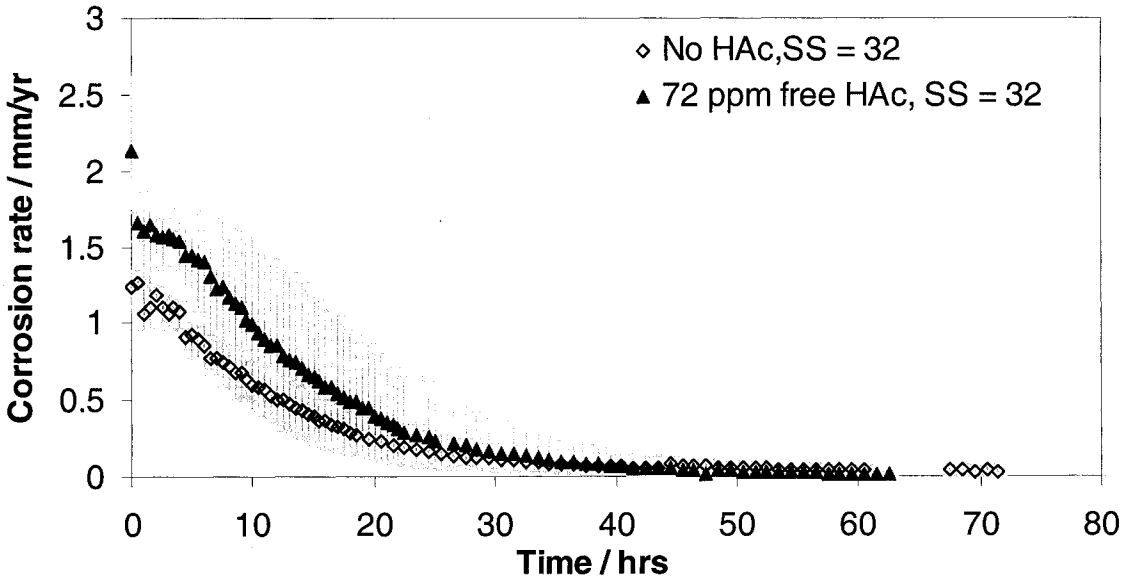

FIGURE 17: Uniform corrosion rate variation with time in experiments without and with 72 ppm free HAc (4000 ppm HAc total) at SS = 32, pH 6.6, 80°C, 10 ppm Fe^{2+}. (Error bars represent the maximum and minimum values of corrosion rate observed. Refer to Figure 18 for the curves shown on a logarithmic scale, Figure 19 for SEM front view and Figure 20 for SEM cross-sectional view.)

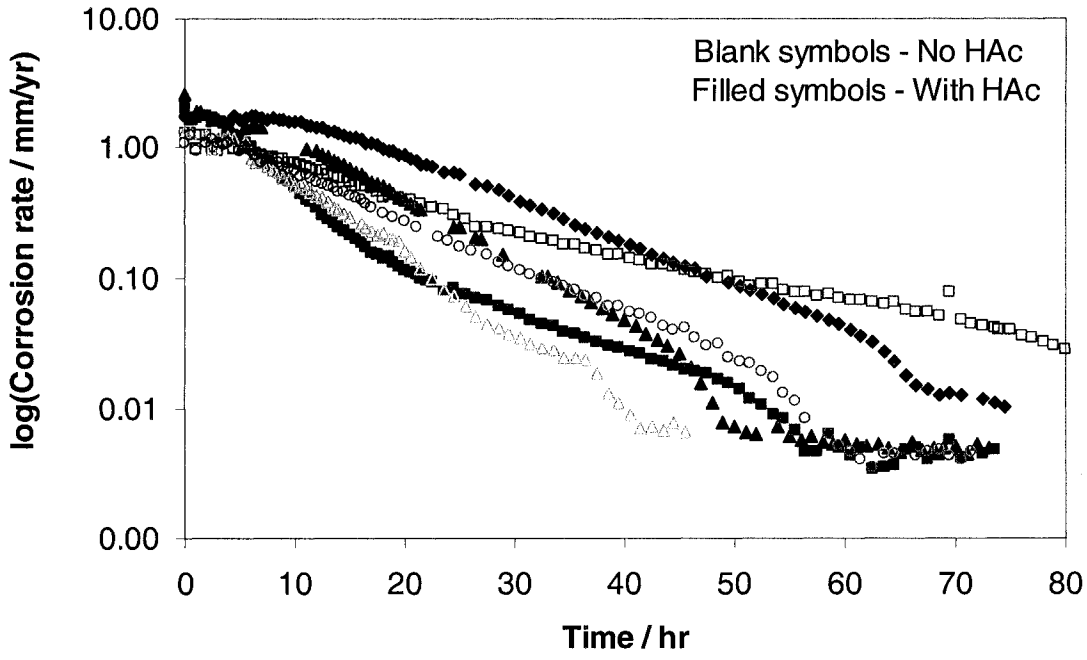

FIGURE 18: Uniform corrosion rate progression with time shown on a logarithmic scale at SS = 32, pH 6.6, T = 80°C, 10 ppm Fe^{2+}, without and with 72 ppm free HAc (4000 ppm HAc total), stagnant conditions. (Refer to Figure 17 for the same curves shown on a linear scale, Figure 19 for SEM front view and Figure 20 for SEM cross-sectional view.)

a) SEM pictures (frontal view) at 1500 X

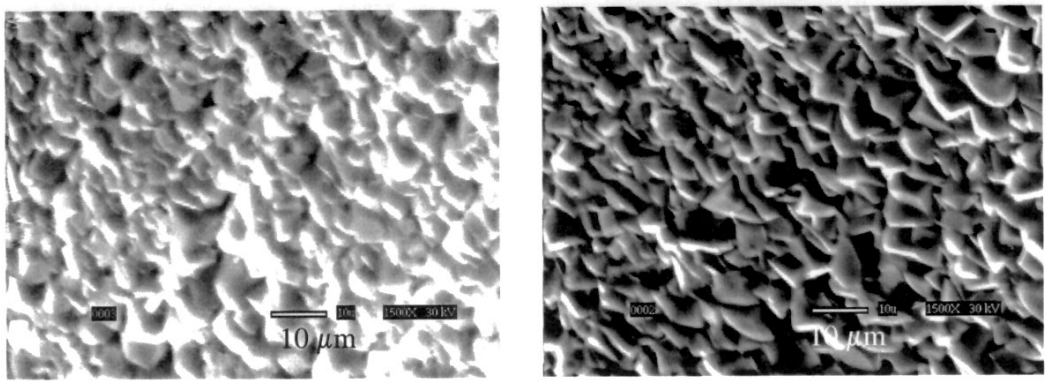

Without HAc

With 72 ppm free HAc

b) Optical microscope pictures at 600X

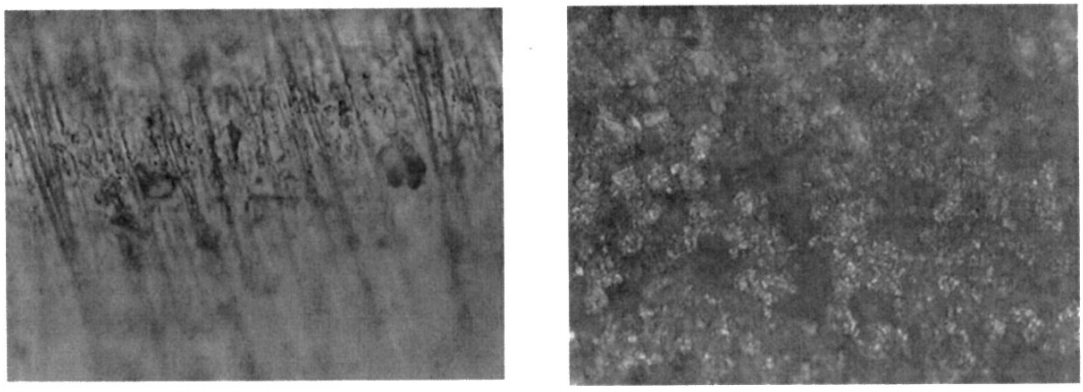

Scale removed (without HAc)

Scale removed (with 72 ppm free HAc)

FIGURE 19: Front view pictures of $FeCO_3$ scale at SS = 32, pH 6.6, 80°C, 10 ppm Fe^{2+}, without and with 72 ppm free HAc (4000 ppm HAc total), stagnant condition. (Refer to Figure 17 for the uniform corrosion rate curves shown on a linear scale, Figure 18 for curves on the logarithmic scale, Figure 20 for SEM cross-sectional view.)

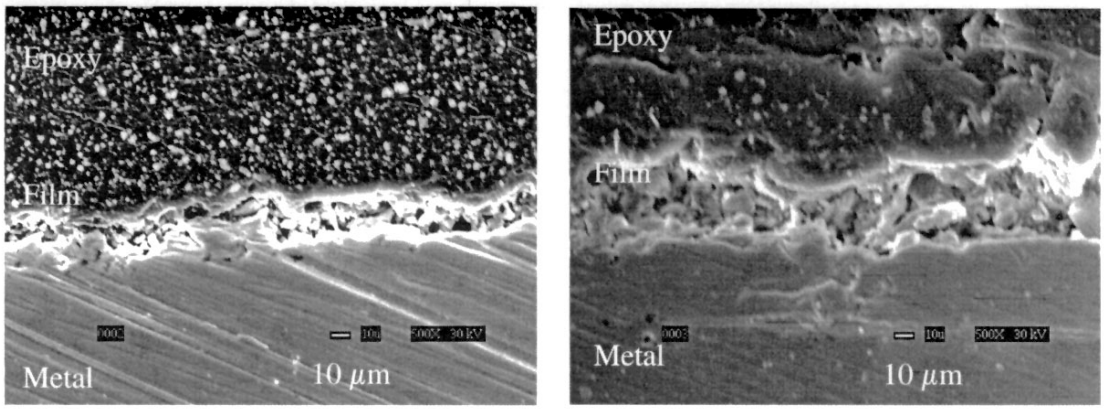

Without HAc With 72 ppm free HAc

FIGURE 20: SEM pictures (cross sectional view) of $FeCO_3$ scale at 500 X, SS = 32, pH 6.6, 80°C, 10 ppm Fe^{2+}, 72 ppm free HAc (4000 ppm HAc total), stagnant condition. Refer to Figure 17 for the uniform corrosion rate curves shown on a linear scale, Figure 18 for curves on the logarithmic scale, Figure 19 for front view.)

b) <u>180 ppm free HAc</u>:

Figure 21 shows the uniform corrosion rates with time for two repeatable experiments each without and with 180 ppm free HAc (10,000 ppm HAc total) at SS = 32, pH 6.6, 80°C, 10 ppm Fe^{2+}. The starting corrosion rate with 180 ppm free HAc is higher than that without HAc resulting in a longer time required to form a protective scale however with no effect on the scale protectiveness. Refer to Figure 22 for the same data shown on a logarithmic scale. Figure 23a shows the front view pictures of the scale at 1500X and also with the scale removed at 600X to look for localized attack. The size of crystals is larger than those observed without HAc although both offered similar corrosion protection. No evidence of localized attack is observed as seen from Figure 23b. Figure 24 shows the SEM cross-section pictures at 500X. Again the thicknesses of scales formed without and with HAc and the final corrosion rate are not distinguishable.

Figure 25 shows the comparison of the uniform corrosion rate curves at SS = 32, without and with 72 and 180 ppm free HAc on a logarithmic scale. There is no significant or systematic effect of HAc on the protectiveness of the scale i.e. on the final corrosion rates. The presence of HAc systematically results in an increase of the initial bare steel corrosion rate resulting in a longer time it requires to form a scale.

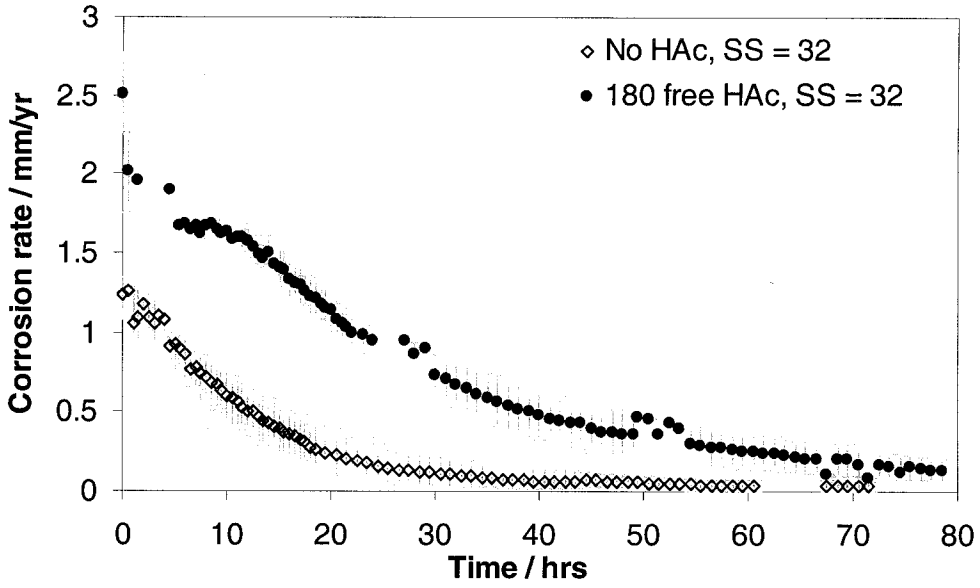

FIGURE 21: Uniform corrosion rate variation with time in experiments without and with 180 ppm free HAc (10,000 ppm HAc total) at SS= 32, pH 6.6, 80°C, 10 ppm Fe^{2+} (Error bars represent the maximum and minimum values of corrosion rate observed, refer to Figure 22 for the curves shown on a logarithmic scale, Figure 23 for SEM front view and Figure 24 for SEM cross-sectional view.)

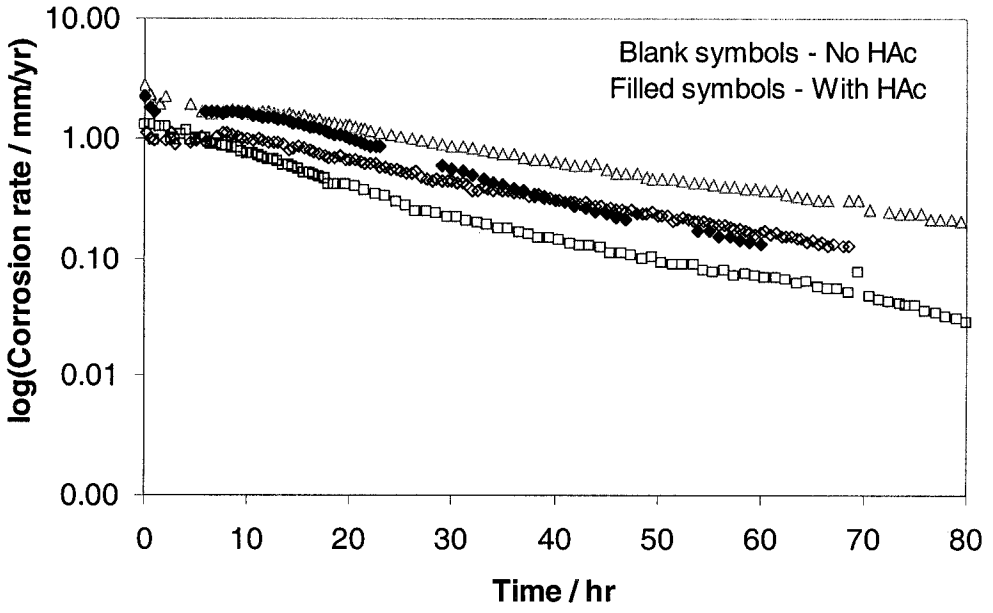

FIGURE 22: Corrosion rate progression with time in the logarithmic scale at SS = 32, pH 6.6, T = 80°C, 10 ppm Fe^{2+}, without and with 180 ppm free HAc (10,000 ppm HAc total), stagnant conditions. (Refer to Figure 21 for the same curves on a linear scale, Figure 23 for front view and Figure 24 for SEM cross-sectional view.)

a) SEM pictures (frontal view) at 1500 X

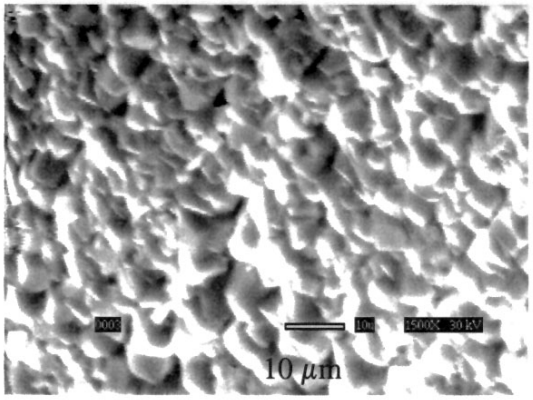

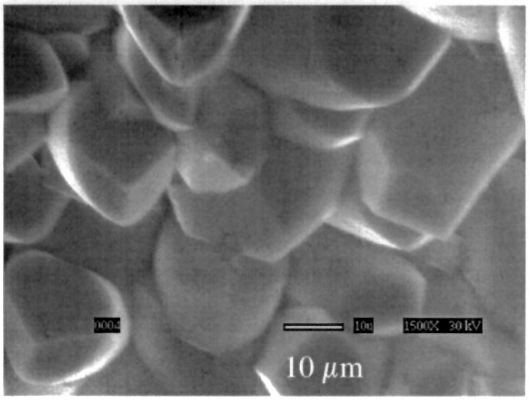

Without HAc

With 180 ppm free HAc

b) Optical microscope pictures at 600X

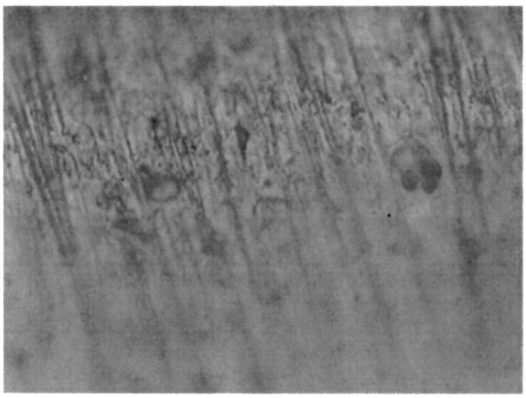

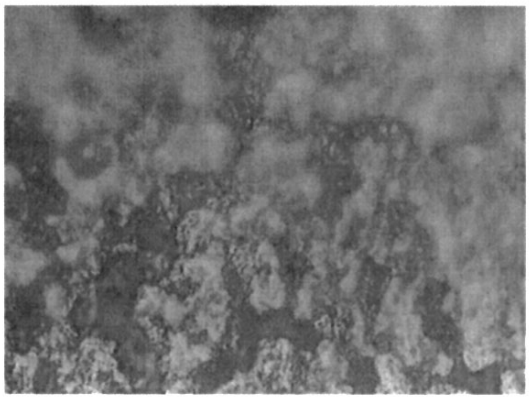

Scale removed (without HAc)

Scale removed (with 180 ppm free HAc)

FIGURE 23: Front view pictures of $FeCO_3$ scale at SS = 32, pH 6.6, 80°C, 10 ppm Fe^{2+}, without and with 180 ppm free HAc (10,000 ppm HAc total), stagnant condition. (Refer to Figure 21 for the uniform corrosion rate curves shown on a linear scale, Figure 22 for the curves shown on a logarithmic scale, Figure 24 for SEM cross-sectional view)

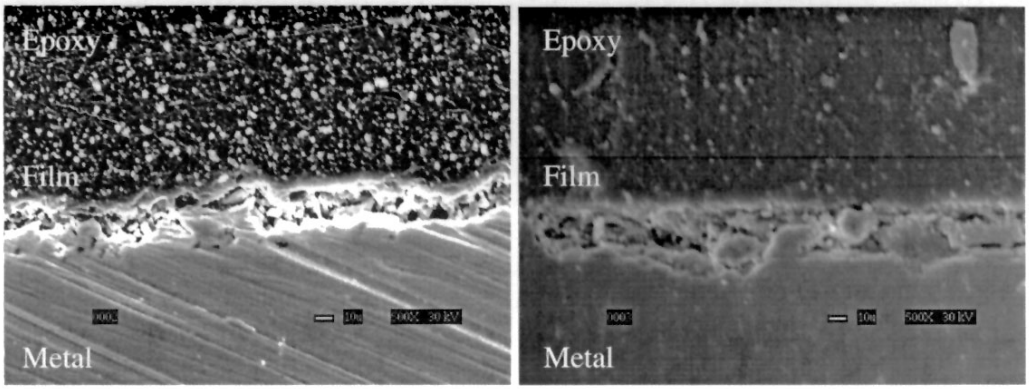

Without HAc With 180 ppm free HAc

FIGURE 24: Front view pictures of $FeCO_3$ scale at SS = 32, pH 6.6, 80°C, 10 ppm Fe^{2+}, without and with 180 ppm free HAc (10,000 ppm HAc total), stagnant condition. (Refer to Figure 21 for the uniform corrosion rate curves shown on a linear scale, Figure 22 for the curves shown on a logarithmic scale, Figure 23 for SEM cross-sectional view).

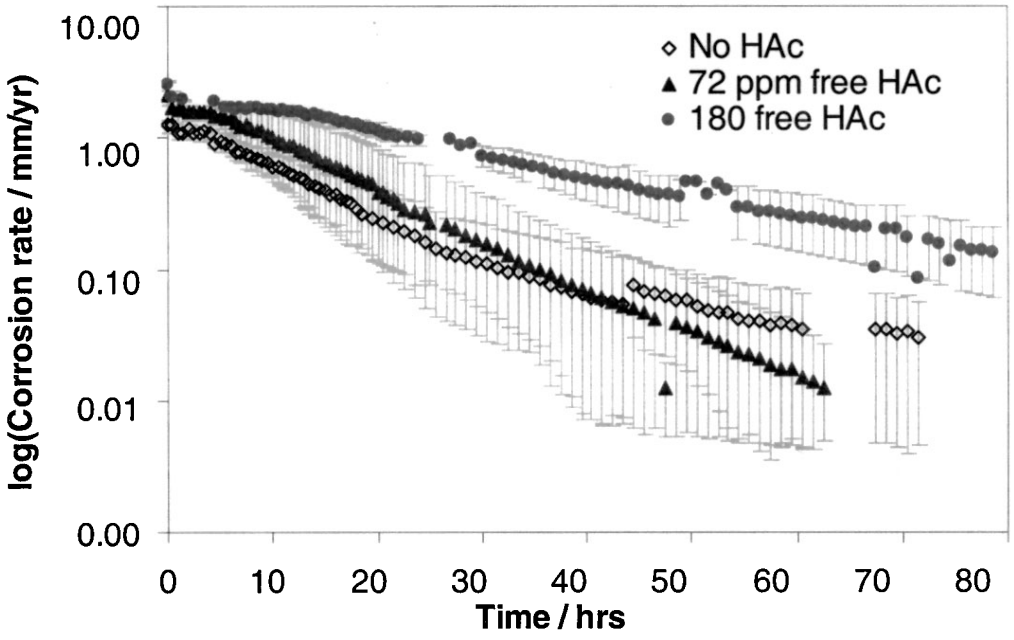

FIGURE 25: Comparison of the uniform corrosion rate curves at SS = 32, pH 6.6, 80°C, 10 ppm Fe^{2+}, with 72 and 180 ppm free HAc, stagnant condition in the logarithmic scale.(Error bars represent maximum and minimum values of corrosion rates.)

Last but not least, it was important to show that the scale observed is indeed $FeCO_3$. We can see from the Pourbaix diagram at the range of pH (6-6.6) and temperature (80°C) that $FeCO_3$ is the only thermodynamically stable species. In order to see the $FeCO_3$ spectrum and match it with the kind of scale observed, an XRD scan was conducted as shown in Figure 26. We can see a good match with the theoretical $FeCO_3$ spectrum[20], confirming the presence of a $FeCO_3$ scale. The extra peak observed at a Bragg's angle of 45° was found[20] to be of carbon.

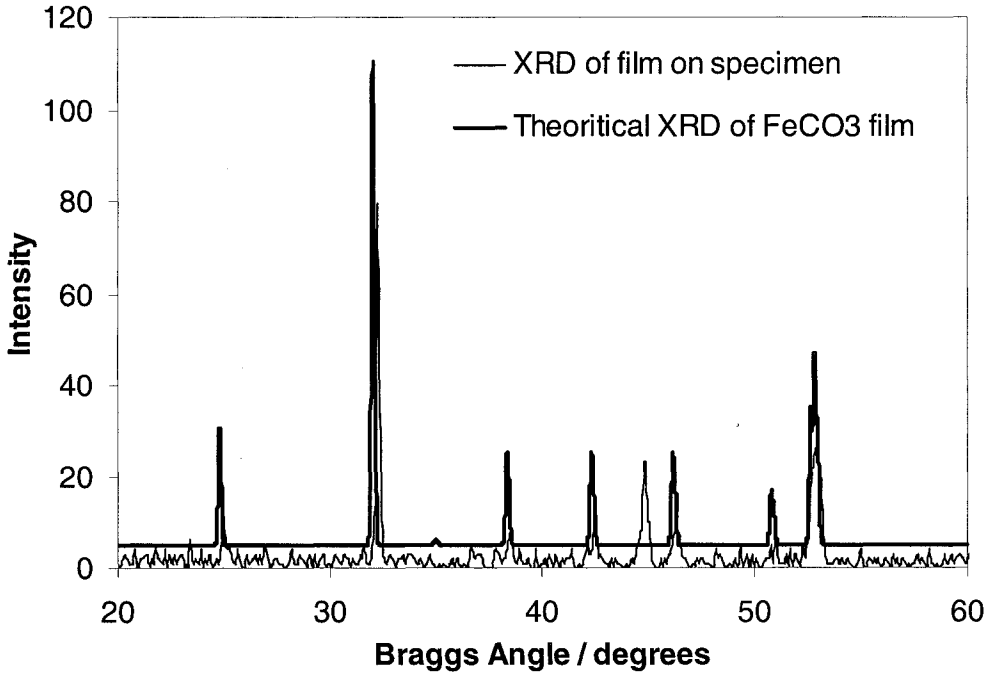

FIGURE 26: XRD Spectrum of protective scale showing it to be iron carbonate.

Measurement of scale porosity using the weight loss/gain method:

The weight of the scale was measured in experiments without HAc and an estimate of the scale porosity was obtained. ASTM Standard Practice G1[19], for cleaning removing the scale using Clarke's solution was followed. Assuming a density of $FeCO_3$ of 3960 kg/m^3, and by accounting for the 15-20 μm thick scale observed by SEM at SS=162, the porosity of scale was calculated to be roughly 50±10%. The porosity at SS = 32 was calculated to be 60±10%.

DISCUSSION

The protectiveness of an iron carbonate scale depends primarily on the rate of precipitation what in turn is a function of temperature and supersaturation as shown by equations (6). At a fixed temperature, the supersaturation is a function of Fe^{2+} and CO_3^{2-} ions concentrations as shown by equation (5). Thus for a given water chemistry (T, pH, pCO_2, etc. all fixed) the concentrations of Fe^{+} and CO_3^{2-} ions is constant irrespective of the amount of HAc present (within the limit

of ideal solutions). Therefore it is not expected that the presence of HAc should affect supersaturation of iron carbonate and the formation or protectiveness of iron carbonate scales. This was borne out by the results of this study where all the important parameters were maintained constant throughout the experiments. The key variable is the pH, which affects both iron carbonate supersaturation as well as the amount of free HAc as discussed at the beginning of this paper.

For a more comprehensive overview of the experimental results that includes experiments conducted at SS of 41 and 10, pH 6.3 and 6 in the presence of 35 and 68 ppm free HAc respectively, for scale integrity experiments at SS of 162 in the presence of 72 ppm free HAc and for the comparison with MULTICORP Version 3.0 corrosion model see reference 18.

CONCLUSIONS

The effect of free HAc on iron carbonate scale formation and protectiveness has been studied in a glass cell, at two different iron carbonate supersaturation values of 162 and 32 at stagnant conditions. A range of free HAc concentrations was tested: 18, 72 and 180 ppm. All experiments were done at a pH 6.6 and temperature of 80°C. The important findings which emerge from this study are:

- While the concentration of free (undisocciated) HAc affects the bare steel CO_2 corrosion rate significantly, there is no significant effect of HAc on iron carbonate scale formation and its protectiveness. Iron carbonate scale thickness, structure and crystal size are virtually unaffected by the presence of HAc.
- There was no evidence of localized corrosion.

REFERENCES

1. Y. Garsany, D. Pletcher and B. Hedges, "The Role of Acetate in CO_2 Corrosion of Carbon steel: Has the Chemistry Been Forgotten?", NACE *Corrosion* 2002, Denver, CO, Paper No. 02273.
2. Y. Garsany, D. Pletcher and B. Hedges, "Speciation and Electrochemistry of Brines Containing Acetate Ion and Carbon Dioxide", *Journal of Electroanalytical Chemistry,* 2002, 538-539, pg 285-297.
3. Y. Sun, K.George, S. Nesic, "The effect of Cl^- and Acetic Acid on Localized CO_2 Corrosion in Wet Gas Flow", CORROSION/2003, Paper No. 03327, (Houston, TX: NACE International, 2003)
4. J.L. Crolet, N. Thevenot, A. Dugstad, "Role of Free Acetic Acid on the CO_2 Corrosion of Steels", NACE *Corrosion* 1999, San Antonio, TX, Paper No. 24.
5. K.George, S.Nesic and C.deWaard, "Electrochemical Investigation and Modeling of Carbon Dioxide Corrosion of Carbon Steel in the Presence of Acetic Acid", NACE *Corrosion* 2003, Houston, TX, Paper No. 04379.
6. S.Wang, K.George and S.Nesic, "High Pressure CO_2 Corrosion Electrochemistry and the Effect of Acetic Acid", NACE *Corrosion* 2004, Houston, TX, Paper No. 04375.
7. K.George, S.Wang, S.Nesic and K.deWaard, "Modeling of CO_2 Corrosion of Mild Steel at High Pressures of CO_2 and in the Presence of Acetic Acid", NACE *Corrosion* 2004, Houston, TX, Paper No. 04623.
8. Y. Garsany, D. Pletcher and B. Hedges, "The Role of Acetate in CO_2 Corrosion of Carbon steel: Studies Related to Oilfield Conditions", NACE *Corrosion* 2003, Houston, TX, Paper No. 03324.
9. M. Joosten, J. Kolts, Justin W. Hembree and M. Achour, "Organic Acid Corrosion in Oil and Gas Production", NACE *Corrosion* 2002, Houston, TX, Paper No. 02294.
10. B. Hedges and L.McVeigh, "The Role of Acetate in CO_2 Corrosion: The Double Whammy", NACE *Corrosion* 1999, Houston, TX, Paper No. 21.
11. J.L. Crolet, M.Bonis, "The Role of Acetate Ions in CO_2 Corrosion", CORROSION/1983, Paper No. 160, (Anaheim, CA: NACE International, 1983)
12. Y.K. Kharaka, "Solmineq 88: A Computer Program for Geochemical Modeling of Water-Rock Interactions", Alberta Research Council, Menlo Park, CA, 1989.
13. M.L. Johnson, M.B. Thomson, "Ferrous Carbonate precipitation kinetics and its impact on CO_2 Corrosion", CORROSION/1991, Paper No. 268, (Cincinnati, OH: NACE International, 1991)
14. Van Hunnick E.W.J., B.F.M. Pots and E.L.J.A.Hendriksen, "The Formation of Protective $FeCO_3$ Corrosion Product Layers in CO_2 Corrosion" CORROSION/1996, Paper No. 6, (Houston, TX: NACE International, 1996)
15. A. Ikeda, M.Ueda, S. Mukai, "CO_2 Behavior of Carbon and Cr Steels", Advances in CO_2 Corrosion- Ed. R.H. Hausler. (Houston, TX, NACE International, 1984)
16. Videm, A. Dugstad, "Corrosion of Carbon Steel in Aqueous CO_2 environment", *Materials Performance,* March 1989, p 63-67.
17. A.Dugstad, "The Importance of $FeCO_3$ Super-saturation on CO_2 Corrosion of Carbon Steels" CORROSION/1992, Paper No.14, (Houston, TX: NACE International, 1992)
18. O.A. Nafday, Master of Science (M.S.) Thesis, August 2004.
19. G.S. Haynes and R. Baboian, Ed, *Laboratory Corrosion Tests and Standards*, ASTM Special Publication 866, 1983, p 505-509.
20. International Center for Diffraction Data (ICDD) Database, Powder Diffraction File (Inorganic phases, alphabetic index) 1989.